

Design and Static Analysis of Feet-legs Device of a Natatores-like Amphibious Robot

Xinru Lin^{1,3}, Liwei Shi^{1,3*}, Shuxiang Guo^{2,3,4}

1.School of Medical Technology, Beijing Institute of Technology, Beijing, 100081, China

2.School of Life Science, Beijing Institute of Technology, Beijing, 100081, China

3.Key Laboratory of Convergence Medical Engineering System and Healthcare Technology(Beijing Institute of Technology), Ministry of Industry and Information Technology, Beijing, 100081, China

4.The Department of Electronic and Electrical Engineering, Southern University of Science and Technology, Shenzhen, Guangdong 518055, China

linxinru@bit.edu.cn, shiliwei@bit.edu.cn, guoshuxiang@bit.edu.cn

*Corresponding author

Abstract - With the increased demand for the exploration of the ocean, the focus of research in the field of robotics has changed. Amphibious robots show broad application prospects. In order to design an amphibious robot adapted to multiple environments, a feet-legs device inspired by natatores was designed. Each webbed foot is made up of three sets of four-linked rods that allow the toe bones to fold and shrink, enabling better imitation of the webbed feet motion of natatores paddling. In order to analyse and optimize the mechanical strength of the critical components of the device during operation, static analysis and structural improvements are made to the webbed feet and the roller of the cylindrical cam. The results show that the static strength of improved webbed feet and the cam roller meet the requirements.

Index Terms - amphibious robot, natatores-like, webbed feet, static analysis, ANSYS.

I. INTRODUCTION

With the exploration of marine resources, especially coastal environments, traditional robots accustomed to a single environment cannot meet the human needs. Amphibious robots show broad application prospects in military and civilian fields.

Bionics provides new design ideas and working principles from an engineering perspective, allowing robots to gain the ability to complete more challenging tasks [1]-[3]. For example, Velox robot, inspired by stingray, can march on the ground, underwater, beach and snow [4]. Guo et al. [5]-[7] designed a turtle-like spherical robot with a real-time detection and tracking system, which not only can realize the transition between quadrupedal crawling and water propulsion movement modes without manual operation, but also can achieve ramp crawling on land. Karakasiliotis et al. [8] designed a salamander-like robot with 27 degrees of freedom which can dynamically scale to accomplish basic motor behavior underwater and on land. Liljeback et al. [9] designed a snake-like robot which is not only capable of swimming underwater, but also of sensing contact forces in the environment. Meng et al. [10] designed a manta-like robot with pectoral fins based on a modified crank rocker mechanism that enables adjust pitch angle rapidly. Shi et al.

[11] designed a robot with a shape memory alloy which was inspired by jellyfish and butterfly and attained a maximum swimming speed of 57.2 mm/s at 24 V. A multi DOF biomimetic robot with a type of biomimetic locomotion employing ionic polymer metal composite actuators was designed, which can realize multiple motions [12].

In addition, bionic robots based on webbed feet paddling have also received some attention. Pandey et al. [13] analysed the mechanism of frog swimming, and designed a frog-like robot with five phalanges connected by a crank-slider mechanism to expand and fold the web. Tang et al. [14] designed a frog-like soft robot with feet actuators capable of increasing the projected area under high voltage, swimming at an average speed of 19 mm/s under a square wave voltage of 5 kV and 0.25 Hz. Kashem et al. [15],[16] designed a duck-like robot whose feet webs connected by double hinges can open automatically with the help of water pressure when the feet move forward, and close automatically when the feet move backward. Liu et al. [17] designed a natatores-like robot whose phalanges could be closed by slider connection, and designed the movement patterns of land and underwater. Chen et al. [18]-[20] designed a beaver-like robot, whose webbed feet can be bent by cable drive to reduce the resistance in the retraction phase, performed dynamical modeling of swimming posture, and accomplished reinforcement learning control for the swimming motions.

Mechanical analysis is of great importance in the design and optimization process of robots. Static analysis of critical components provides a basis for designing more rigid structures [21]. Niu et al. [22] performed static and modal analyses of critical components of a natatores-like amphibious robot which provide a basis for the optimization of structure.

To sum up, scholars have made great achievements in amphibious bionic robots, but there are few bionic robots based on webbed feet, which can face the complex space environment exploration tasks. In this study, a feet-legs device is designed, with slider four-link webbed feet inspired by natatores, which can achieve the folding and closing of the toe bones when the foot moves forward, and the opening of the toe bones when the foot moves backward. Static analyses are also

performed on critical components. The dangerous positions are optimized in structure, to meet the requirement of motion.

The structure of the rest of the paper is as follows. Section II describes the bionic principle based on natatores-like motion. Section III describes the mechanical design of the feet-legs device. Section IV describes the static analysis of the critical components. Section V describes the conclusion and the future work.

II. BIONIC PRINCIPLE

The hind limb of natatores is mainly composed of femur, tibia, metatarsus and toe bones. To design feet-legs device inspired by natatores, it is necessary to analyse the principle of natatores motion in water and on land.

A. The Bionic Principle in Water

The principle of feet propulsion of natatores is considered to be resistance-based swimming. Johansson et al. [23] found that when natatores swim at very high speeds, the feet move through the water at a more appropriate angle, and that drag-based propulsion actually uses hydrodynamic forces as the primary source of forward thrust. The swimming motion of natatores can be divided into diving motion and surface swimming motion. Diving motion is characterized by webbed feet parallel paddling to provide the main propulsion to overcome buoyancy. A paddling cycle can be divided into three phases: power phase, glide phase and recovery phase [24]. Surface swimming motion is characterized by webbed feet alternating paddling. A paddling cycle can be divided into two phases: power phase and recovery phase. Fig.1 shows that in the power phase the web between toe bones is fully expanded to increase the overflow area when foot sweeps backward in an arc, and in the recovery phase the web is folded to reduce the response resistance [25]. In order to get faster swimming speed, natatores obtain greater propulsion during the power phase by changing the area of the web, and reduce water resistance during the recovery phase.

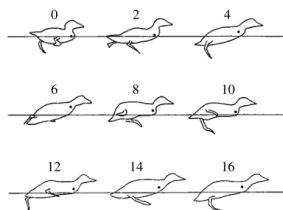


Fig. 1. Natatores' flapping motion for water skiing [25]

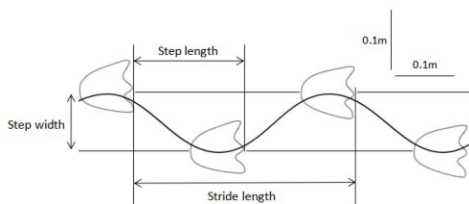


Fig. 2. Natatores walking track and its center of gravity moving curve [26]

B. The Bionic Principle on Land

Fig.2 shows natatores walking track and its center of gravity moving curve. To prevent falling, natatores have larger gravity center amplitude range and smaller stride length, showing the motion posture of rocking forward [26]. The abilities of natatores to swim in the water and walk in the mud are worth learning, even though the walking posture of natatores is not perfect.

III. MECHANICAL DESIGN

After observing the natatores limb structure and motion, the mechanical structure of a natatores-like feet-legs device is designed, which has the characteristics of environmental adaptability and concealment.

Fig.3 shows the overall structure of feet-legs device. The design of mechanical system includes the webbed feet design, cylindrical cam design and leg design. The two legs and feet are identical in structure, distributed on both sides of the body, and each group is composed of a femur, tibia, metatarsus, toe bones, hip joint and knee joint, as shown in Fig.4.

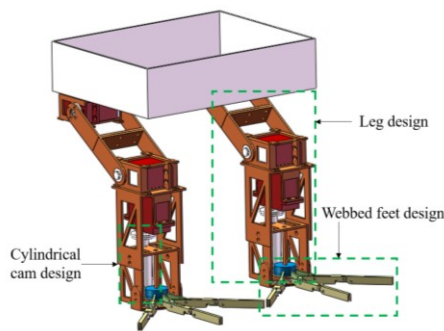


Fig. 3. Overall structure of feet-legs device

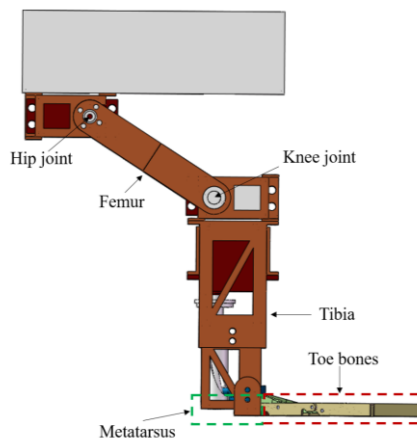


Fig. 4. Side view of feet-legs device

A. Webbed Feet Design

The webbed feet have three toe bones, connected together by a middle slider, with rubber membrane covering each toe bone to simulate the web of natatores, as shown in Fig.5. Each toe bone is composed of a set of slider four-link structure, in order to make the toe bone folded. The four-rod linkage mechanism is simple to build, which is easy to machining and

can bear large loads meeting the force need in the motion of natatores-like robot.

The slider moves downward to drive three toe bones unfold away from the central slider, driving the web on the toe bones to unfold, increasing the projected area and the water propulsion. The phase of webbed feet changes from Fig.5(b) to Fig.5(a).

The slider moves upward to drive three toe bones bend and fold toward the central slider, driving the web on the toe bones to fold, reducing the projected area and the water resistance. The phase of webbed feet changes from Fig.5(a) to Fig.5(b).

The fins are made of flexible material, which can be extended to 2-3 times the initial area.

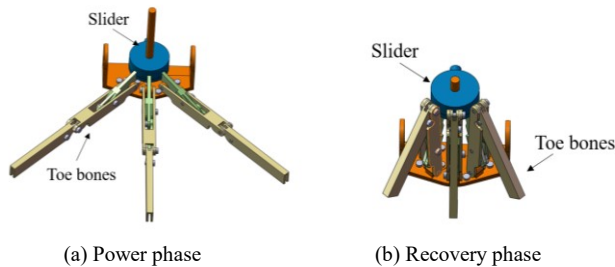


Fig. 5. Webbed feet design

B. Cylindrical Cam Design

Slider crank mechanism, gear rack mechanism, ball screw and cam mechanism are both able to transform rotary motion into linear motion. However, cylindrical cam is chosen with more compact structure, considering the working space, waterproof and control.

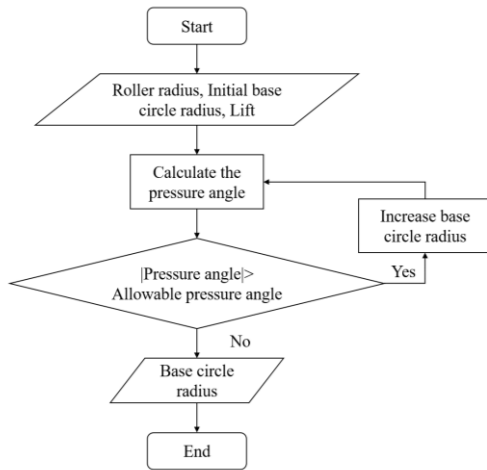


Fig. 6. Flow chart of cylindrical cam design

In order to design a cylindrical cam with the smallest size within the allowable pressure angle, the radius of the base circle is calculated. Fig.6 shows the flow chart of cylindrical cam design. Input parameter of roller radius, initial base circle radius and lift, to calculate the pressure angle. If the calculated pressure angle is greater than the allowable pressure angle, the radius of base circle will be increased by 1 mm, until the pressure angle is not greater than the allowable pressure angle,

at which point the result of base circle radius is output. The cam obtained with this base circle radius is the optimal one in the ideal case.

The calculation shows the minimum radius of the base circle that satisfies the maximum pressure less than the allowable pressure angle. The minimum curvature meets the condition of being greater than 0.35 times the roller radius, when the roller will work properly and the actual profile will not be sharpened or distorted.

The obtained theoretical contour lines are imported into the software for modeling. It can be manufactured by CNC (Computer numerical control) machining. The selection of a waterproof servo motor to drive the cylindrical cam meets the need for webbed feet control during the fold and unfold motion.

C. Legs Design

Fig.7 shows the three dimensional graph of legs design. The hip and knee joints each have 1 degree of freedom and are each driven by a waterproof servo motor. The hole design of legs helps reduce water resistance.

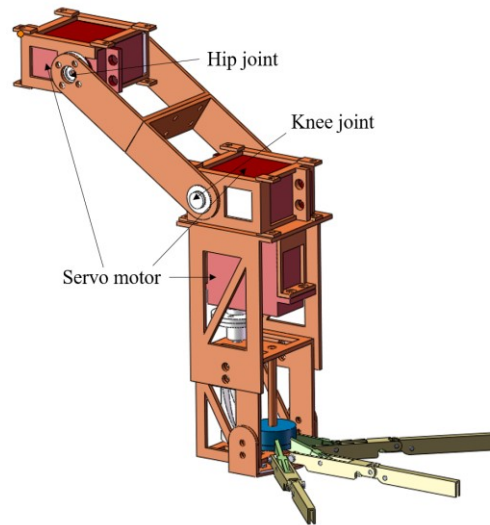


Fig. 7. Legs design

IV. STATIC ANALYSIS

The feet-legs device must have enough sufficient strength to bear the load in different working conditions. In order to ensure that the device cannot fail during operation, strength analysis of critical components is required. The working condition that the maximum force is applied to the webbed feet and roller of cylindrical cams is analysed in this section. The “static structural” module of ANSYS Workbench software is used for finite element model establishment and static simulation calculation.

A. Webbed Feet

Ribak et al. [27] calculated and measured the vertical force on the paws of adult cormorants during swimming in a tank at room temperature during a motion cycle, and found that the force was less than 15N. The vertical force of 20N

applied to the toe bones was chosen for strength analysis, considering the impact.

Fig.8 shows the three dimensional elastoplastic finite element model of webbed feet, which uses structural steel. The material properties are shown in Table I. The safety factor is 2, and allowable stress is 125MPa. Tetrahedron is selected as the element type, and 40873 elements and 76530 nodes are divided in total. The circular hole of the frame is applied fixed support. The vertical force of 20N applied to the surface of the toe bones. Bonded contact is applied to the contact surface between parts that can produce relative displacement, and the value of the coefficient of friction is 0.17. Fixed contact is applied to contact surface between other parts.

Fig.9 shows the distributing graph of the equivalent stress at the webbed feet. The value of maximum equivalent stress is 706MPa, which is much greater than the allowable stress of structural steel. The positions of drive rods, support frame, shaft on the slider and holes of shaft are dangerous. The webbed feet will be fail in these positions during motion.

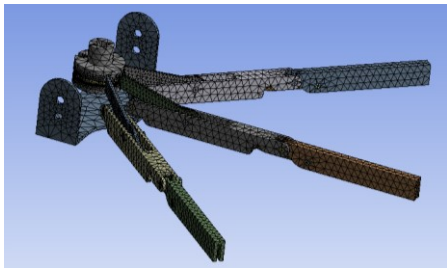


Fig. 8. Three dimensional elastoplastic finite element model of webbed feet

TABLE I
THE MATERIAL PROPERTIES OF STRUCTURAL STEEL

Properties	Value
Density	7850kg/m ³
Young's Modulus	200GPa
Poisson's Ratio	0.3
Yield Strength	250MPa

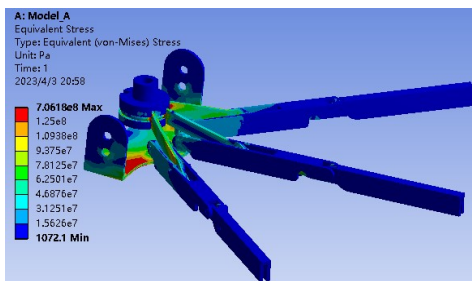


Fig. 9. Distributing graph of the equivalent stress at the webbed feet

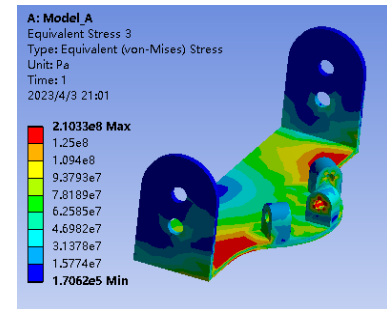
Fig.10 shows the distributing graph of the equivalent stress at the dangerous positions. The maximum equivalent stress occurs at the connection position of the drive rod to the shaft on the slider, with value of 674MPa, and the strength around other holes also does not meet the requirements, as shown in the Fig.10(a). The maximum equivalent stress occurs at the bottom of the support frame, with value of 210MPa, as shown in the Fig.10(b). The maximum equivalent stress occurs at the connection with the drive rod, due to structural irrationality, with value of 371MPa, as shown in the Fig.10(c).

The holes of other shaft also bear equivalent stress, which beyond allowable stress.

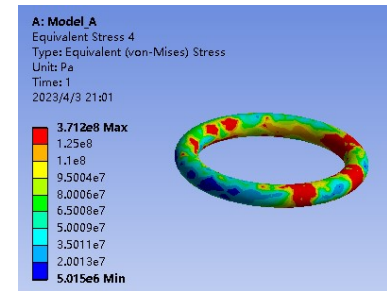
In order to make the webbed feet meet the strength requirements during the working process, structural improvements are made to the dangerous positions. The shape and size of the drive rods on both sides are changed. The support frame structure is changed, from a whole to an assembly, and its thickness is increased. The connection of the shaft on the slider is changed, from exposed steel wire to three steel shafts inside the slider. The length and radius of the holes are changed.



(a) Drive rods



(b) Support frame



(c) Shaft on the slider

Fig. 10. Distributing graph of the equivalent stress at the dangerous positions



Fig. 11. Three dimensional elastoplastic finite element model of optimized webbed feet

Fig.11 shows three dimensional elastoplastic finite element model of optimized webbed feet, which uses structural steel. Tetrahedron is selected as the element type, and 98890 elements and 164492 nodes are divided in total. The circular hole of the frame is applied fixed support. The vertical force of 20N applied to the surface of the toe bones. The types of connect are the same as the settings of webbed feet before optimized.

Fig.12 shows the distributing graph of the equivalent stress at the optimized webbed feet. The maximum equivalent stress occurs at the contact position of the transmission rod and toe bone. The value is 117MPa, which is less than allowable stress of structural steel, so the strength of optimized webbed feet meets the requirement.

Fig.13 shows the distributing graph of the equivalent stress at the optimization dangerous positions. The maximum stress on the drive rod changes from 674MPa to 84MPa. The maximum stress on the support frame changes from 210MPa to 89MPa. The maximum stress on the support frame changes from 371MPa to 18MPa. The maximum stresses in dangerous positions are reduced, suggesting that the improvement is effective.

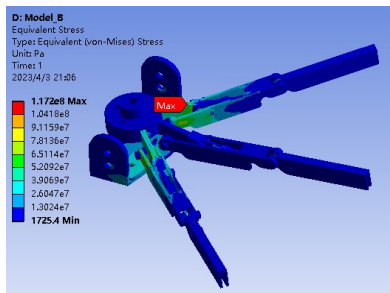
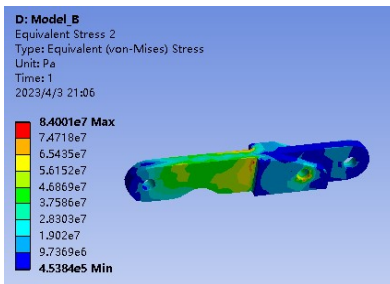
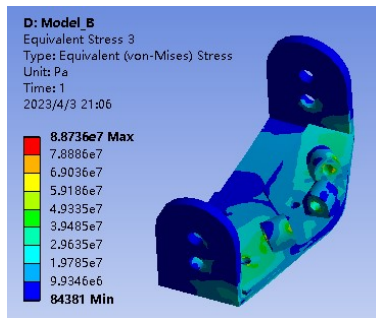


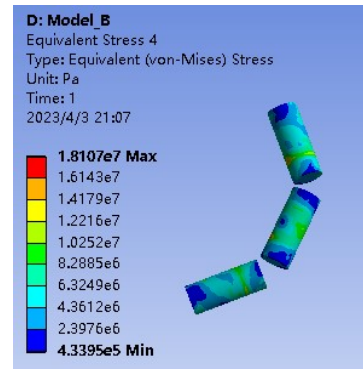
Fig. 12. Distributing graph of the equivalent stress at the optimized webbed feet



(a) Optimized drive rods



(b) Optimized support frame



(c) Optimized shaft in the slider

Fig. 13. Distributing graph of the equivalent stress at the optimized dangerous positions

B. Roller

The roller-slider of the cylindrical cam is assembled instead of using welded parts, considering the difficulty of machining, though the welded parts can bear large force. Fig.14 shows three dimensional elastoplastic finite element model of roller, which also uses the structural steel. The tetrahedron is also used as the element type, and the component is divided into 274598 nodes and 401210 elements in total. Bonded contact is applied to the contact surface roller shaft and slider, because the bolt is used for connection of them. The force is 21.57 N, applied to the surface of the roller, which is determined by the maximum pressure angle of the cylindrical cam and the force applied to the toe bones.

Fig.15 shows distributing graph of the equivalent stress at the roller. The maximum equivalent stress occurs at the connection between the roller shaft and the slider, with the value is 36MPa, which is less than the allowable stress of structural steel. Therefore, the strength of roller can meet the requirement.

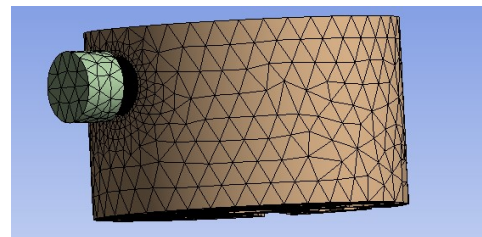


Fig. 14. Three dimensional elastoplastic finite element model of roller

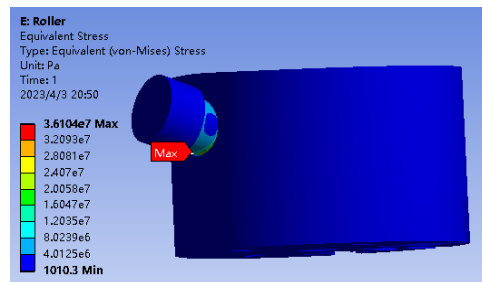


Fig. 15. Distributing graph of the equivalent stress at the roller

V. CONCLUSION AND FUTURE WORK

Based on the principle of bionics, a feet-legs device inspired by natatores is designed. Regarding the mechanical design, 2 degree of freedom legs structure is used to provide more flexible movement, and three sets of four-linked rods are used to simulate the real webbed feet of natatores. The optimal cylindrical cam is calculated to drive the toe bones folding and unfolding. The static analysis of the critical components of the device is carried out. The results show that the strength of the optimized webbed feet and roller meets the requirements. The simulation results lay a foundation for the following optimization design work of the whole natatores-like robot.

The follow-up work should continue to complete the design of the overall structure of the robot. The gait of robot in water and on land should be analysed and designed, and physical experiments should be completed to realize the motion of the robot.

ACKNOWLEDGMENT

This work was supported by National Natural Science Foundation of China (62273042, 61773064).

REFERENCES

- [1] Wang GB, Chen DS, Chen KW, et al., "The current research status and development strategy on biomimetic robot," *Journal of Mechanical Engineering*, vol. 51, no. 13, pp. 27-44, 2015.(in Chinese)
- [2] A. Ramezani, S.-J. Chung, and S. Hutchinson, "A biomimetic robotic platform to study flight specializations of bats," *Sci Robot*, vol. 2, no. 3, p. eaal2505, 2017.
- [3] Hyun Soo Park, S. Floyd, and M. Sitti, "Roll and Pitch Motion Analysis of a Biologically Inspired Quadruped Water Runner Robot," *The International Journal of Robotics Research*, vol. 29, no. 10, pp. 1281-1297, 2010.
- [4] PES (Pliant Energy Systems), Robotics. <https://www.pliantenergy.com/robotics>, 2017.
- [5] S. Guo et al., "Modeling and experimental evaluation of an improved amphibious robot with compact structure," *Robot Cim-int Manuf*, vol. 51, p. 37-52, 2018.
- [6] Xing Huiming, Guo Shuxiang, et al., "A Novel Small-scale Turtle-inspired Amphibious Spherical Robot," *2019 IEEE/RSJ International Conference on Intelligent Robots and Systems (IROS)*, pp. 1702-1707, 2019.
- [7] Guo Shuxiang, Pan Shaowu, et al., "A system on Chip-Based Real Time Tracking System for Amphibious Spherical Robots," *International Journal of Advanced Robotic Systems*, vol. 14, no. 4, pp. 1-19, 2017.
- [8] K. Karakasiliotis et al., "From cineradiography to biorobots: an approach for designing robots to emulate and study animal locomotion," *J. R. Soc. Interface.*, vol. 13, no. 119, p. 20151089, 2016.
- [9] P. Liljebäck, O. Stavdahl, K. Y. Pettersen, and J. T. Gravdahl, "Mamba - A waterproof snake robot with tactile sensing," *2014 IEEE/RSJ International Conference on Intelligent Robots and Systems (IROS)*, pp. 294-301, 2014.
- [10] Y. Meng, Z. Wu, H. Dong, J. Wang, and J. Yu, "Toward a Novel Robotic Manta With Unique Pectoral Fins," *IEEE Trans. Syst. Man Cybern, Syst.*, vol. 52, no. 3, pp. 1663-1673, 2022.
- [11] Shi Liwei, Guo Shuxiang, Asaka Kinji, "A Novel Jellyfish-And Butterfly-Inspired Underwater Microrobot with Pectoral Fins," *International Journal of Robotics And Automation*, vol. 27, no. 3, pp. 276-286, 2016.
- [12] Shi Liwei, Guo Shuxiang, Asaka Kinji, "A Novel Multifunctional Underwater Microrobot," *2010 IEEE International Conference on Robotics and Biomimetics (ROBIO)*, pp. 873-878, 2010.
- [13] J. Pandey, N. S. Reddy, R. Ray, and S. N. Shome, "Biological swimming mechanism analysis and design of robotic frog," *2013 IEEE International Conference on Mechatronics and Automation (ICMA)*, pp. 1726-1731, 2013.
- [14] Y. Tang, L. Qin, X. Li, C.-M. Chew, and J. Zhu, "A frog-inspired swimming robot based on dielectric elastomer actuators," *2017 IEEE/RSJ International Conference on Intelligent Robots and Systems (IROS)*, pp. 2403-2408, 2017.
- [15] S. Kashem and H. Sufyan, "A novel design of an aquatic walking robot having webbed feet," *Int J Autom Comput*, 2017.
- [16] S. B. A. Kashem, S. Jawed, J. Ahmed, and U. Qidwai, "Design and Implementation of a Quadruped Amphibious Robot Using Duck Feet," *Robotics*, vol. 8, no. 3, p. 77, 2019.
- [17] H. Liu et al., "Hydrodynamic Analysis of Webbed Foot for a Novel Biomimetic Robotic Duck," *2019 IEEE International Conference on Advanced Robotics and its Social Impacts (ARSO)*, pp. 45-50, 2019.
- [18] G. Chen, X. Ti, L. Shi, and H. Hu, "Design of Beaver-like Hind Limb and Analysis of Two Swimming Gaits for Underwater Narrow Space Exploration," *J Intell Robot Syst*, vol. 104, no. 4, p. 65, 2022.
- [19] G. Chen, W. Peng et al., "Modeling of swimming posture dynamics for a beaver-like robot," *Ocean Engineering*, vol.279, no.114550, 2023.
- [20] G. Chen, Y Liu et al., "Reinforcement learning control for the swimming motions of a beaver-like, single-legged robot based on biological inspiration," *Robotics and Autonomous Systems*, vol. 154, no. 104116, 2022.
- [21] S. Guo et al., "Modal and fatigue analysis of critical components of an amphibious spherical robot," *Microsyst Technol*, vol. 23, no. 6, pp. 2233-2247, 2017.
- [22] Y. Niu, L. Shi, and S. Guo, "Static and Modal Analysis of Critical Components of a Natatores-like Amphibious Robot," *2022 Youth Academic Annual Conference of Chinese Association of Automation (YAC)*, pp. 1554-1559, 2022.
- [23] L. C. Johansson and R. Å. Norberg, "Delta-wing function of webbed feet gives hydrodynamic lift for swimming propulsion in birds," *Nature*, vol. 424, no. 6944, pp. 65-68, 2003.
- [24] G. Ribak, J. G. Swallow, and D. R. Jones, "Drag-Based 'Hovering' in Ducks: The Hydrodynamics and Energetic Cost of Bottom Feeding," *PLoS ONE*, vol. 5, no. 9, p. e12565, 2010.
- [25] T. L. Aigeldinger and F. E. Fish, "Hydroplaning by Ducklings: Overcoming Limitations to Swimming at the Water Surface," *Experimental Biology*, vol. 198, no. 7, pp. 1567-1574, 1995.
- [26] H. Liu, L. Shi, S. Guo, H. Xing, X. Hou, and Y. Liu, "Platform Design for a Natatores-like Amphibious Robot," *2018 IEEE International Conference on Mechatronics and Automation (ICMA)*, pp. 1627-1632, 2018.
- [27] G. Ribak, D. Weihs, and Z. Arad, "How do cormorants counter buoyancy during submerged swimming," *J Exp Biol*, vol. 207, no. 12, pp. 2101-2114, 2004.